

An 8x1 Sierpinski Carpet Fractal linear Array Antenna design for Multiband Applications

K.S Chakradhar¹ Dr.B.Rama Rao² Dr.D.Nataraj³ Dr.N.Gireesh⁴ Dr.K.Chitambar Rao⁵

¹ Assoc.Professor, Sree Vidyanikethan Engineering College, Tirupati, India

² Professor, Aditya Institute of Technology and Management, Tekkali, India

³ Assoc.Professor, Pragati Engineering College, Kakinada, India

⁴ Professor, Sree Vidyanikethan Engineering College, Tirupati, India

⁵ Assoc.Professor, Aditya Institute of Technology and Management Tekkali, India

Abstract-Single element antennas in many applications can not satisfy the demands of gain or radiation pattern. A potential alternative may be to incorporate several antenna components in an array. In this article, novel fractal structure-based array antenna architecture, Fractal arrays used to maximise the antenna's bandwidth and reduce the grid lobes, has been identified. The proposed antenna is usable throughout the 3.1GHz to 10.6 GHz range explicitly reserved for the UWB applications. The proposal involves an 8-element print fractal linear array antenna for wireless communication and multiband deployment working on frequencies between 2.2GHz and 12GHz through minimal ground plane rather than complete ground plane. The Sierpinski Carpet Framework for 2nd Iteration used for the Fractal linear Array configuration of the antenna. He also addresses the Fractal linear antenna architecture measures. The 8- elements linear array and Fractal linear array are designed, simulated and tested by using Vector network analyser and the simulation and the practical results are compared.

Key words: Microstrip Patch, Linear array, Fractal linear Array, Multiband.

I. INTRODUCTION

Antennas have been an essential resource in recent years, and through the development of telecommunications networks. Modern telecommunication networks need a larger antenna with narrower measurements and wider bandwidth. Antennas with very directing characteristics (very high gain) must be configured for certain applications. This can be done by the Antenna array [1]. Normally, single-element antenna radiation patterns are extreme large, i.e. they would be low guidance (good). Antennas with high directivity are also needed in long-distance communication. This method will therefore result in the presence of numerous lateral lobes. These antennas can be built by broadening the width of the radiated gap (maximum size much greater than τ). In comparison, the antenna is normally wide and hard to produce. The elements of the table are typically the same. It's not really needed, but practical and easy to design and manufacture. The multiple elements (wire dipoles, loops, holes etc.) may be very different. The full array is the vector overlay of the fields of each variable. It is also necessary to interfere in the partial fields in the desired direction and to interfere destructively with the remaining environment in order to achieve very directive models. The overall pattern of the antenna is governed by five fundamental strategies: 1. the geometric array arrangement (circular, linear, rectangular, spherical, etc.), 2. The virtual position of the items 3. The excitation amplitude of each component 4. Each element's excitation phase, 5. Every element 's individual pattern.

Fractal arrays

A fractal is a self-similar shape with a non-integer dimension [2]. Self-like suggests that a significant portion of the shape will have the same composition like the whole geometry. Fractals were first applied to antenna arrays by Kim and Jaggard [3]; and since then, several analysis and synthesis techniques for fractal arrays have been developed [4,5]. Fractal arrays could be generated by using a repeating generator to construct a slightly larger, identical array. In the design and analysis of arrays, the fractal principle may be used by either evaluating the array with fractal theory or putting elements inside fractal modules or taking all of those elements into account [12]. Fractal array entity arrangement can generate a slim array and achieve multi-band efficiency. Random fractal properties have been used to establish a concept strategy for quasi-random fractals. The generation of array configurations between totally ordered (this is, periodic) and totally disordered (e.g., regular) was used as regular fractals too. The key benefit of this strategy is that it produces sparse arrays that have comparatively low side lobes, which are linked to periodical arrays, but not to random arrays, but still durable [10] [4]. A collection of non-uniform arrays, called Weierstrass arrays would have the property that the distance between their elements and present distributions could be self-scaled and repetitively generated. Synthesis techniques based on the self-scalability properties for fractal radiation patterns have also been developed. The generator array has a pattern that is replicated, scaled and interpreted several times. The definition of fractal may either be used to analyse the array using fractal theory, or to position elements in fractal structures or both in the design and in the study of arrays. Fractal array entity arrangement can generate a thin range and conduct multi-band. Examples include the linear array of the cantor, the cantor ring array and the planar array of the Sierpinski carpet [6].

II. SIERPINSKI CARPET FRACTAL ANTENNA DESIGN

The Sierpinski Carpet fractal could be defined using eight specific affine transformations W_j which are initially applied to the unit square S_0 [12] $S_0 = \{ (x_1, x_2) \in \mathbb{R}^2 / (x_1 \geq 0), (x_1 \leq 1), x_2 \geq 0, x_2 \leq 1) \}$

$$W_1 = [1/3, 0, 0, 1/3, 0, 0]$$

$$W_2 = [1/3, 0, 0, 1/3, 0, 1/3]$$

$$W_3 = [1/3, 0, 0, 1/3, 0, 2/3]$$

$$W_4 = [1/3, 0, 0, 1/3, 1/3, 2/3]$$

$$W_5 = [1/3, 0, 0, 1/3, 2/3, 2/3]$$

$$W_6 = [1/3, 0, 0, 1/3, 2/3, 1/3]$$

$$W_7 = [1/3, 0, 0, 1/3, 2/3, 0]$$

$$W_8 = [1/3, 0, 0, 1/3, 1/3, 0]$$

The first three iterations of Sierpinski carpet antenna $i=0,1,2$, are shown in Fig. 1

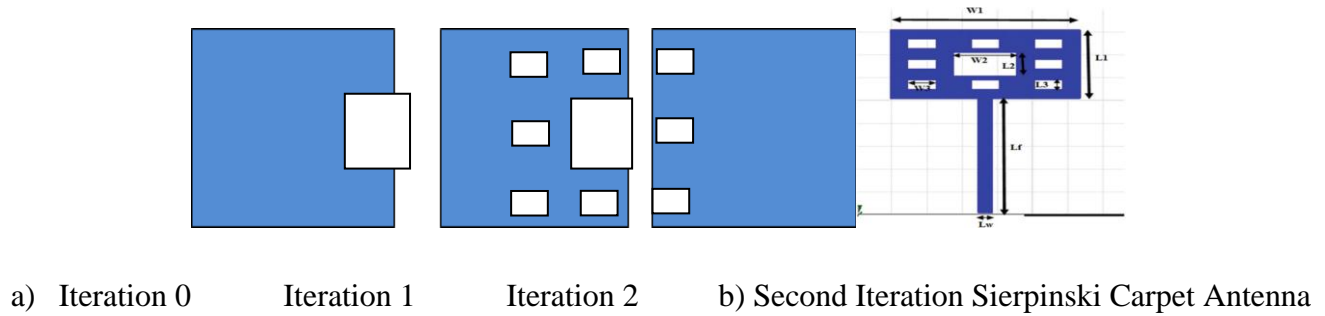


Fig.1 Iteration stages of Sierpinski Carpet Fractal antenna

The algorithms based on the affine transformations are capable of generating the geometry of both types of antennas. They have been implemented as completely parameterized models for the 3D conformal FDTD electromagnetic simulator. The models were used to calculate the return-loss, resonant frequency, VSWR and gain parameters. The antenna architecture focuses on a single element that use the simple microstrip square patch antenna. Length L and width W are calculated by using equations (3.1), (3.3), (3.5), and (3.7). The antenna dimensions are calculated by using the *Transaction-level modelling* (TLM) Model. The width of the Microstrip Patch Antenna is given by [1]

$$w = \frac{c}{2f \sqrt{\frac{\epsilon_r + 1}{2}}} \quad (1)$$

ϵ_{reff} , the Effective Dielectric constant is defined as

$$\text{for } \frac{w}{h} \geq 1 \quad \epsilon_{\text{reff}} = \frac{\epsilon_r + 1}{2} + \frac{\epsilon_r - 1}{2} \left[1 + 12 \frac{h}{w} \right]^{-\frac{1}{2}} \quad (2)$$

$$\text{for } \frac{w}{h} \leq 1 \quad \epsilon_{\text{reff}} = \frac{\epsilon_r + 1}{2} + \frac{\epsilon_r - 1}{2} \left[1 + 12 \frac{h}{w} \right]^{-\frac{1}{2}} + 0.041 \left[1 - \sqrt{\frac{w}{h}} \right] \quad (3)$$

The patch measurements are expanded to incorporate the fringing effects into consideration. The extension shall be provided by,

$$\Delta L = 0.412h \frac{(\epsilon_{\text{reff}} + 0.3) \left(\frac{w}{h} + 0.264 \right)}{(\epsilon_{\text{reff}} - 0.258) \left(\frac{w}{h} + 0.8 \right)} \quad (4)$$

The effective length is generated by, as the length was being increased to either side of the patch,

$$L_{\text{eff}} = \frac{c}{2f \sqrt{\epsilon_{\text{reff}}}} \quad (5)$$

Patch resonant length L shall be calculated by,

$$L = L_{\text{eff}} - 2\Delta L \quad (6)$$

Patch Input impedance is calculated by the formula

$$R_{in} = \frac{1}{2(G_1 \pm G_{12})} \quad (7)$$

Where

$$G_{12} = \frac{1}{120\pi^2} \int_0^\pi \left[\sin \left[\frac{k_0 W \cos \theta}{2} \right] / \cos \theta \right]^2 J_0(k_0 L \sin \theta) \sin^3 \theta d\theta$$

$$G_1 = \frac{I_1}{120\pi^2}$$

$$I_1 = \int_0^\pi \left[\sin \left(\frac{k_0 W \cos \theta}{2} \right) / \cos \theta \right]^2 \sin^3 \theta d\theta$$

$$k_0 = (2 * \pi) / \lambda$$

The Inset Depth of the antenna y_0 is calculated by the formula

$$R_{in}(y=0) = \frac{1}{2(G_1 \pm G_{12})} \cos^2 \left(\frac{\pi y_0}{L} \right) \quad (8)$$

The Characteristic Impedance of the antenna is given by

$$Z_0 = \frac{60}{\sqrt{\epsilon_{eff}}} \ln \left[\frac{8h}{W_0} + \frac{W_0}{4h} \right] \text{ for } \frac{W_0}{4h} \leq 1 \quad (9) \quad Z_0 = \frac{120\pi}{\sqrt{\epsilon_{eff}} \left[\frac{W_0}{h} + 1.393 + 0.667 \ln \left(\frac{W_0}{h} + 1.44 \right) \right]}$$

$$\text{for } \frac{W_0}{h} \leq 1 \quad (10)$$

Where W_0 is the strip width

The notch width g is calculated by

$$g = \frac{v_0}{\sqrt{2 \times \epsilon_{eff}}} \frac{4.65 \times 10^{-12}}{f} \quad (11)$$

The inset width S is given by

$$S = (2 * g) + W_0 \quad (12)$$

The ground plane dimensions are determined as the following

Ground plane length

$$L_g = 6h + L \quad (13)$$

Ground plane width

$$W_g = 6h + W \quad (14)$$

Patch Antennas and Feed Mechanisms

The configuration collection facilitates less power gain and much less efficiency to be overcome. When constructing an array, the structure of the feed network is critical. Consequently, the size and process of

each element might well be flexibly governed by the feed structure. Parallel feed, power divider T-Split, Wave Quarter and Bend Mitered feeds are separate feed network modes.

There are two main criteria in the configuration of the linear array

- i) The two components are distinguished in the antenna panel is equal to the $\lambda/2$ distance.
- ii) The power division regulations should be expanded to feed each antenna feature.

The antenna for the wavelength of 4 GHz is calibrated to achieve a distance of 75 mm and 37.5 mm with a distance of 37.5 mm from each device.

$$\lambda = \frac{3 \times 10^8}{4 \times 10^9} = 0.075m = 7.5cm$$

$$\lambda/2 = 37.5 \text{ mm}$$

A linear array of 8×1 is the structure the antenna. The HFSS Linear Array antennas model appears in Fig. 1, a number of antenna components are designed from a FR4 substrate of a dielectric constant of 4.4. The substratum length = 10 cm and substrate width is 30.00. 1. The Antenna comprises of eight monitor components divided by 37.5 mm.

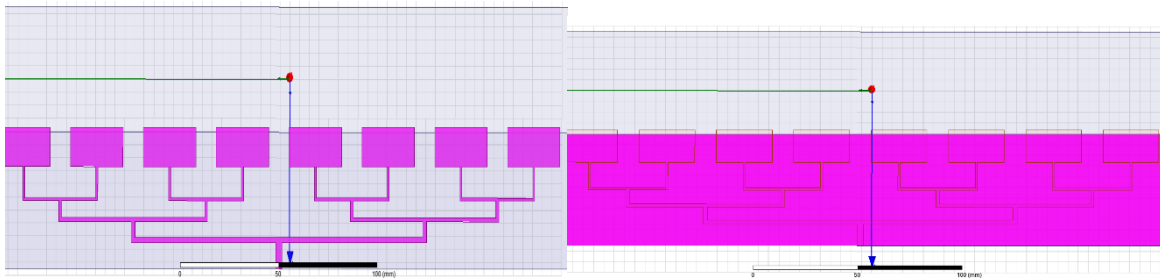


Fig. 2. a) HFSS design model of Linear array b) Ground plane

The antenna has been designed for partial ground rather than a full ground plane. Well after iterations, the base standard was defined at a length of 52 mm and a width of 300 mm. In Figure 2 the HFSS result indicates partial ground.

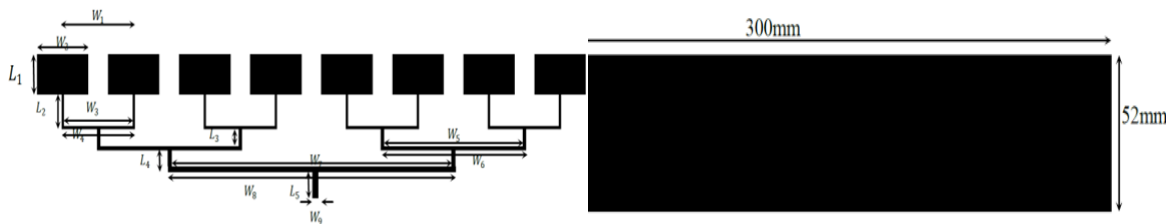


Fig. 3. a) Dimensions of linear array b) Ground plane

It is indeed a 50Ω micro strip transmission line finished on a $\epsilon_r=4.38$ substratum and 1.6 mm in height. The configuration of the expected monopoly antenna with absolute ground plane of the micro strip transmission is shown in Fig . 4. The antenna is equipped with a 50Ω micro strip line and assembled on the FR4 substratum with a thickness of 1.6 mm. The structure and composition of fractals to the rectangles is a smooth, rectangular structure. The pulsating element is fed by a 50Ω micro band

transmission line which does have a centre width of = 3 mm and is attached to the measurement by the subminiature A (SMA) connector. The whole ground plane has been used on back of a substratum. The ground level measurements written on its back are $W \times L$ where $W=30$ cm and $L=10$ cm. The ground level is specified for the foundation. The discrepancy between the irradiating patch and the ground plane is $G = 1.6$ mm. The Ansoft HFSS simulation programme simulated and calibrated the antenna.

The antenna's ideal dimensions are as follows: $W_1=37.5$ mm, $W_2=21$ mm, $w_3=36.5$ mm, $W_4=38.5$ mm, $w_5=73.5$ mm, $W_6=76.5$ mm, $W_7=148$ mm, $W_8=152$ mm, $W_9=3$ mm, $L_1=10$ mm, $L_2=13$ mm, $L_3=8$ mm, $L_4=8$ mm, $L_5=10$ mm.

Table 1: Linear array antenna optimal dimensions

| Parameter | Dimension | Parameter | Dimension | Parameter | Dimension |
|-----------|-----------|--------------|-----------|-------------|-----------|
| W_1 | 37.5mm | W_6 | 76.5mm | $L_2=13$ mm | 13mm |
| W_2 | 21mm | W_7 | 148mm | $L_3=8$ mm | 8mm |
| W_3 | 36.5mm | $W_8=152$ mm | 52mm | $L_4=8$ mm | 8mm |
| W_4 | 38.5mm | $W_9=3$ mm | 3mm | $L_5=10$ mm | 10mm |
| W_5 | 73.5mm | $L_1=10$ mm | 10mm | | |

III. GEOMETRIES AND DESIGN CONCEPTS OF FRACTAL ANTENNA

Sierpinski Carpet Fractal Patch Antenna

The fractal antenna has been at most commonly materialized antenna fractal geometry [18, 19]. Thus the fractal antenna is a type of repetitive geometrical configurations, each with its own specific attributes. The peer-like existence transmitted on this antenna was expected to produce its multi-band function. In the other hand, a conventional antenna can be solved and operates at a single frequency. After the configuration of the zero iteration of Sierpinski geometry the following equations was used to incorporate further iterations

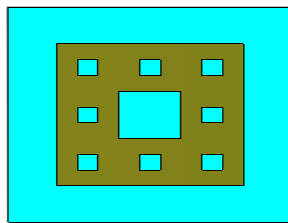


Fig.4 Sierpinski carpet geometry

The designed antenna is 8×1 linear Array. A set of antennas were equipped for the substratum FR4 with a dielectric constant 4.4. The length of the substrate $L_s=10$ cm and the width of the substratum were 30 cm. The antenna is created by 8 array-elements, divided by 37.5 mm. This is also the second iteration of the fractal, the HFSS configuration of the Linear Fractal antenna is defined in Fig.5. The HFSS configuration is a basic linear array.

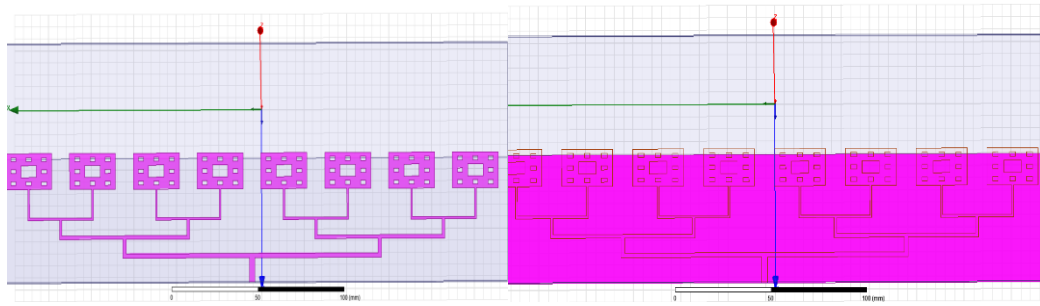


Fig. 5.a) HFSS design of 8-Elemental Linear Fractal array b) Partial ground plane

The antenna gets installed on a minimal ground instead of the entire spectrum. Just after iterations, a length of 52 mm and a width of 300 mm is connected to the ground plane. This means the completed opening line of 50Ω per micro strip engrave with a base of $\epsilon_r=4.38$ and height 1.6 mm is added. Fig.8 displays the configuration of the planned monopoly antenna with absolute ground plane the transmission line fed with micro strips. The antenna is fed onto a 50-inch micro strip line and produced on the 1 / inch thickness FR4 substratum with relative permittiveness of 4.4. The type of the radiating portion is a rectange flat surface with fractal application to the rectangles. The transmission line has a central width = 3 mm and is attached with a sub miniature A (SMA) connector for measuring purposes. The transmission line is fed by 50 bars of the radiation portion. The whole ground plane is used on the back of the substratum. The length of the ground plane prints on the back of the substratum is $W \times L$ where the radiating patch and the ground plane have a difference of $W=30$ cm and $L=10$ cm. The antenna has been tested and calibrated with Ansoft High Frequency Simulator (HFSS) Simulation Program.

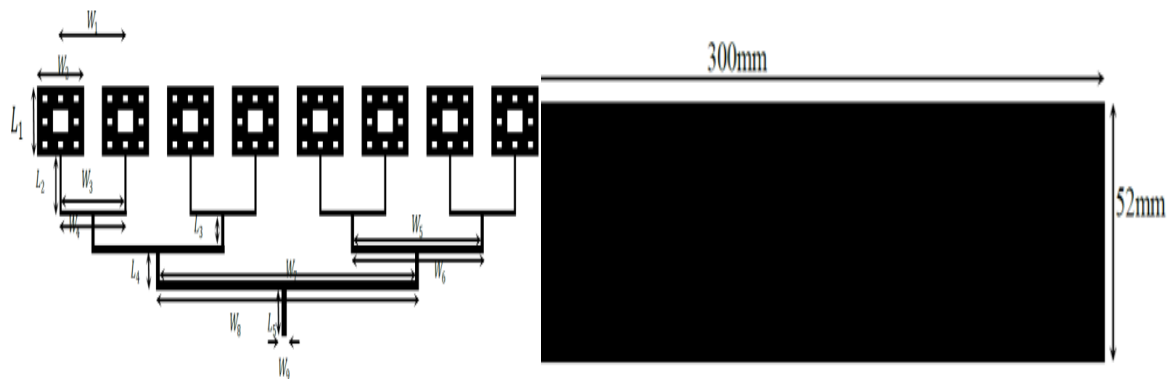


Fig. 6.a) Dimensions of linear Fractal array b)Ground plane

The antenna 's ideal dimensions are as follows: $W_1=37.5\text{mm}$, $W_2=21\text{mm}$, $W_3=6.5\text{mm}$, $W_4=38.5\text{mm}$, $W_5=73.5\text{mm}$, $W_6=76.5\text{mm}$, $W_7=148\text{mm}$, $W_8=152\text{mm}$, $W_9=3\text{mm}$, $L_1=10\text{mm}$, $L_2=13\text{mm}$, $L_3=8\text{mm}$, $L_4=8\text{mm}$, $L_5=10\text{mm}$. In the following figure, the partial framework in the HFSS model was shown. The first fractal iteration dimensions are $W_{f1} \times L_{f1} = 7\text{ mm} \times 3.33\text{mm}$ to rectangular slots. The next fractal iteration consists of $W_{f2} \times L_{f2} = 2.33\text{ mm} \times 1.11\text{ mm}$ rectangular slots. The linear array as well as fractal linear array was both assembled by using above-mentioned measurements of the 1.6 mm diameter FR4 substratum and relative permittivity to 4.4.

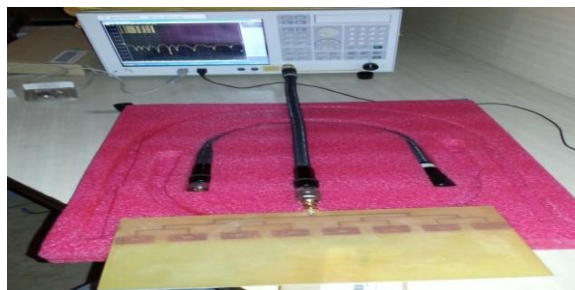


Fig. 7. The Experimental setup for the measurement of linear fractal array

IV. RESULTS AND DISCUSSIONS

i) Simulation results

A. Linear Array Return Loss

The Fig..11 shows the Return Loss obtained for the linear array antenna described above

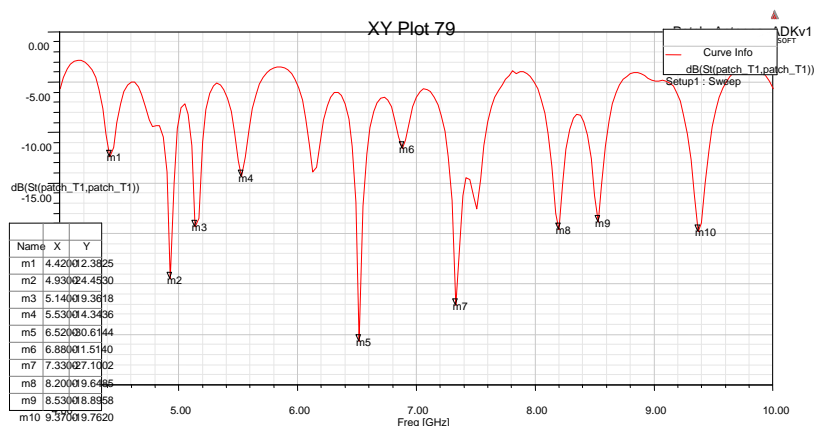


Fig. 8 Linear Array return loss curve

Just like mentioned above, the antenna was configured for 4GHz frequency with a distance of 37.5 mm from the antenna components. The feed network of the antenna is an significant consideration during the design process as the impedances differ and lower the level of the side lobe on the feed network. The initial impedance of 50Ω could not be achieved as the number of array components has risen to 8. The engineered antenna generates a multiband or multi-frequency response due to the differences in impedance, due to changes in the feed network. The antenna displays a return loss higher than -10dB, which is particularly useful since its return loss is -10dB. The Antenna recorded a return loss of -12.38 dB at 4.420 GHz, -19.36 dB at 5.14 GHz, -24.45 dB at 4.93 GHz, -14.34 dB at 5.53 GHz, -11.51 dB at 6.88 GHz, -30.6 dB at 6.52 GHz, -27.10 dB at 7.33 GHz, -19.64 dB at 8.2 GHz, -19.76 dB at 9.37 GHz, -18.89 dB at 8.53 GHz,. One such antenna could be then used to communicate with mobile devices or other applications using these frequencies.

B. Linear Array Antenna Gain

Below is the 2D polar route of the antenna:

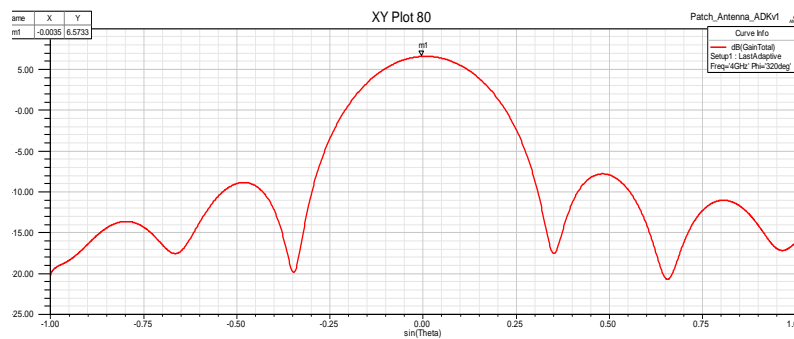


Fig. 9. 2-D gain plot of Linear array

The antenna gain plays a very important role and determines the coverage area and directive properties of the antenna constructed. The prototype antenna has shown a 6.6dB improvement of 4GHz and the above plot defines the 3dB polar plot from -90 to 90 phase variations. In general, the gain over 3dB is recommended for the practical use.

C. Linear Array Side Lobe Levels

The key factor behind the design of the array of antennas is that the lateral lobe levels are decreased and the antenna direction is increased. The smaller the lateral lobe the higher the output of the antenna in the direction sought. The built antenna shows a gain of 7.5 dB. Effective feeding network, since variations in feed network, antenna impedance and efficiency characteristics differ, are the key factors influencing the side lobe levels. The power separator law was implemented for feeding to antenna and feeding to a precisely balanced antenna is made possible by the feed network's lengths and widths. The antenna built revealed a lateral lobe of -15.4dB (Right side lobe) with -14.4dB (left side lobe). Lower the appropriate values of the side lobe of the built antenna are -13.5dB such that the antenna can be used in practical use.

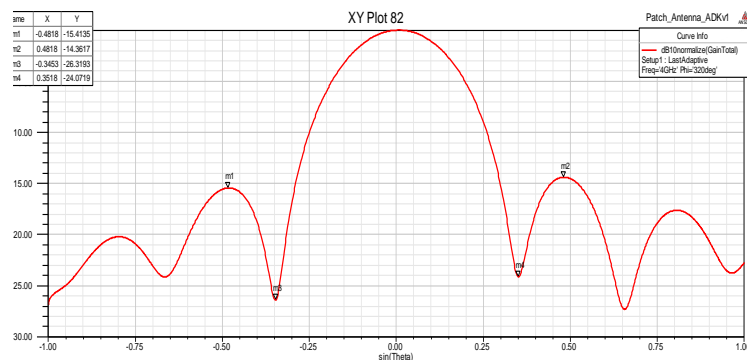


Fig. 10 Side lobe levels plot of Linear array

The antenna's bandwidth is 0.69 and the antenna displays a larger stream. However, the antenna decreased in frequency as the number of elements increased. The sum of antenna elements is inversely commensurate with the antenna bandwidth.

D. Fractal Linear Array Return Loss

Below is the return failure of the above antennas:

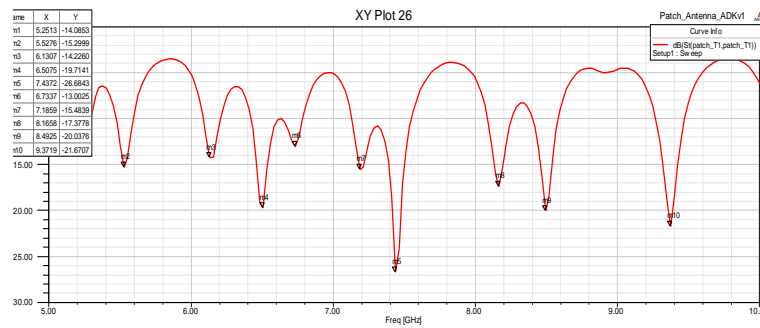


Fig. 11. Return loss curve of Fractal Linear array

The rectangle fractal antenna design is specified with 4GHz frequency, with a gap of 37.5 mm between antenna components, the antenna being different from the initial configuration due to the feed network used to trigger the antenna. With the increase of the number of elements to eight, a difference in the effective feed network length of the built antenna is observed with a cross-band or cross frequency response. Although the ideal return loss is -10dB, it's very handy to use the antenna showing stronger return loss as it passes other constraints. The second instance of the fractal array was added to the linear array: -14.08 dB at 5.25 GHz, -14.22 dB at 6.13 GHz, -15.29 dB at 5.52 GHz, -19.71 dB at 6.50 GHz, -13.00 dB at 6.73 GHz, -26.68 dB at 7.43 GHz, -15.48 dB at 7.18 GHz, -20.03 dB at 8.49 GHz -21.67 dB at 9.37 GHz and -17.37 dB at 8.16 GHz,. This antenna could be implemented to communicate with mobile devices or other applications that run in these frequencies.

E. Fractal Linear Array Antenna Gain

Fig.14 displays the 2D Gain linear fractal array antenna.

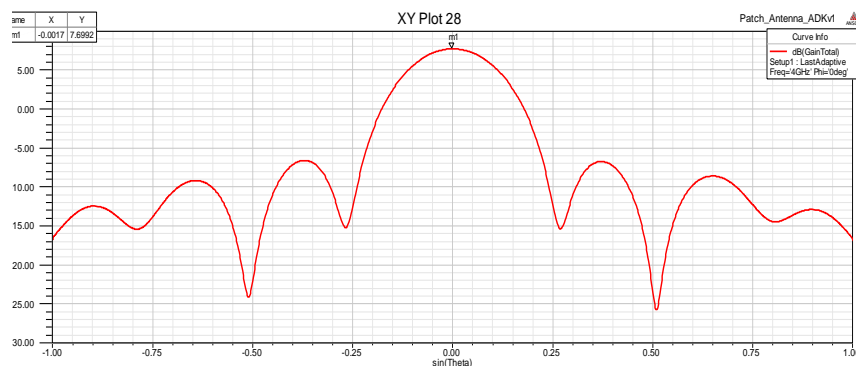


Fig. 12. 2D gain plot of Fractal Linear array

The antenna gain plays a crucial role and determines the coverage area and the directional characteristics of the antenna being constructed. The built antenna obtained 7.7dB at 4GHz and the above plot was defined in the 2D gain plot from -90 to 90 phase variance. For practical use, the gain of over 3dB is ennoblement needed.

F. Fractal Linear Array Side Lobe Levels

The key explanation why antennas are built is that the lateral lobe is reduced and the antenna is more directed. The lower the lateral lobe the higher the output of the antenna in the direction sought. There was a 7.7 dB gain in the built antenna. Efficient feed networks are the key factors influencing lateral lobes, as the differences in the feed network are likely to result in an antenna impedance and differ in efficiency. In the configuration of the ideally paired antenna the power dividing rule was applied for feeding the antenna, the length and width of the feed network. The constructed antenna demonstrated -14,2 dB on the right side and -14,4 dB on the left. The lateral lobe levels in the built antennas are below the appropriate lateral lobe levels -13.5dB in order to allow the antenna to be used in operation.

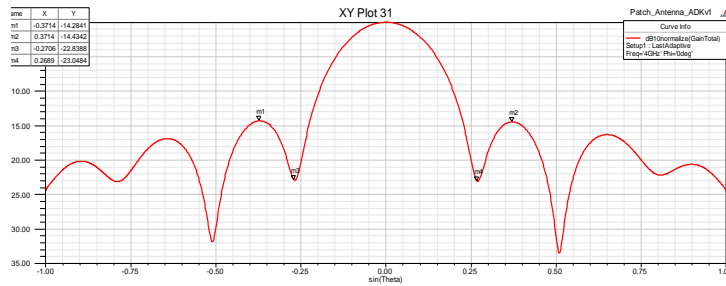


Fig.13. Side lobe levels of Fractal Linear array

The antenna bandwidth is 0.54 suggesting a wider stream. The antenna is 0.54. However, the antenna displayed a drop in bandwidth as the number of elements of the antenna is increased. The sum of antenna elements is inversely commensurate with the antenna bandwidth. The number of antenna elements must be expanded for smaller bandwidth. The linear monitor increases the increase of the number of antenna elements increasing and the beam diameter reduces with the number of antenna elements.

ii). Measured Results

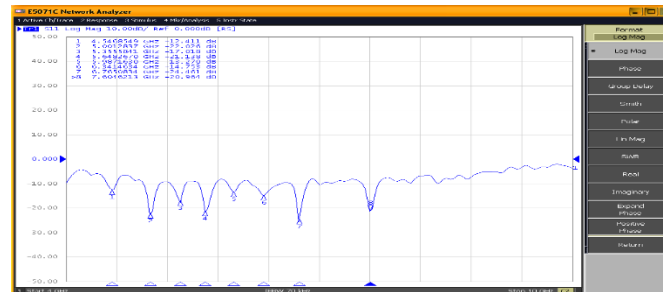


Fig.14 Return loss curve of linear Array Using Vector network Analyzer

The return loss curve of the linear fractal array antenna as seen in figure 6.20. Figure 6.20 indicates that the antenna has resonated with a separate return loss on 8 bands. This antenna can be used for mobile communications with the -12,41dB, -22,02dB, 5,00GHz, -17,01dB 5,35GHz, -21,13dB 5,64 GHz, -13,2dB 5,98GHz, -14,75dB with 6,34 GHz, -24,46dB 6.76 GHz and -20,96dB with 7,60 GHz, -222dB at 5,0GHz. It could be used for mobile communication.



Fig.15 a)Return loss b)VSWR Curve of Linear array Using Vector network Analyzer

The fractal linear antenna of the Sierpinski fabric shown in the diagram. 6.22, return array failure is obtained -19.53dB at 5.55GHz, -22.56dB at 6.14GHz, -28.99dB at 6.54GHz and -18.79 dB at 7.44 GHz, -15.50dB at 8.17 GHz. It can be used for cell communication. This antenna could be used for the mobile communication.

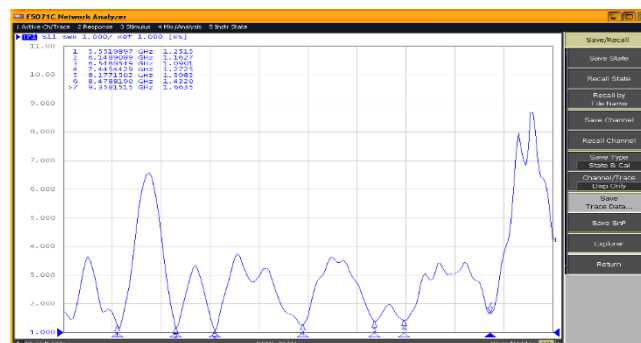


Fig.17 VSWR Curve of Fractal Linear array Using Vector network Analyzer

The VSWR curve is 1.25, 1.16, 1.09, 1.2, 1.39, 1.43 and 1.70. Fig.6.23 is the fractal linear series.

V. COMPARISON SIMULATION AND MEASURED RESULTS

The relationship between the results simulated and the results of the antenna generated effects of the return failure is seen on the figure below. 6.25-6.27. The measured-simulated relation is seen in Table 6.1 Below are the results of the simulation compared with the manufactured antenna results.

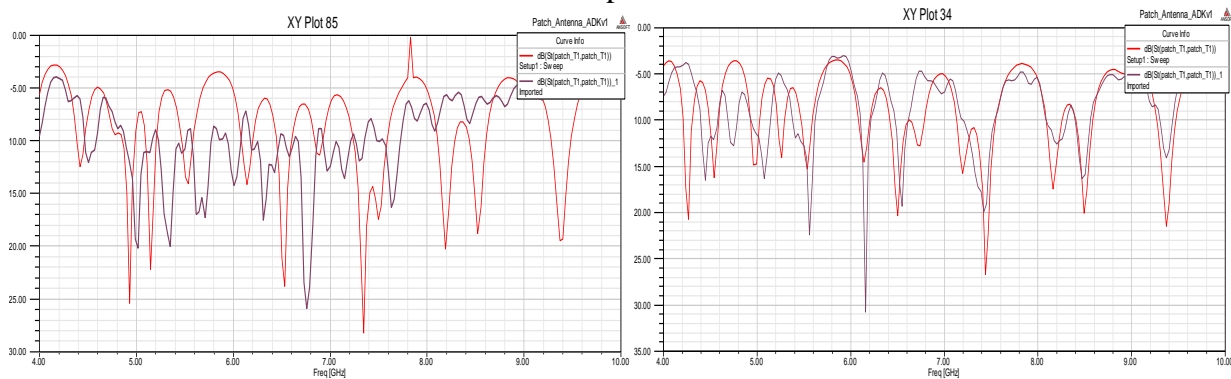


Fig. 18 Return Loss comparison of Linear Array and Fractal Linear Array

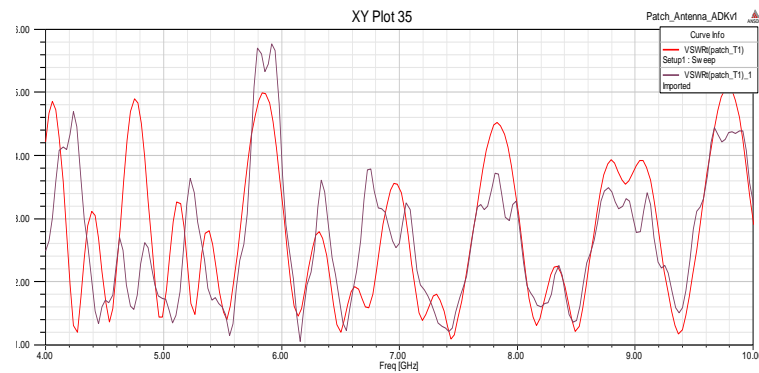


Fig. 20 VSWR Comparison of Fractal Linear Array

Table II Comparison of return loss of Linear array and Fractal linear array

| Linear array | | | | Fractal linear array(dB) | | | |
|--------------------|-----------------|---------------------|-----------------|--------------------------|-------------|---------------------|-----------------|
| Simulated | | Measured | | Simulated | | Measured | |
| Resonant freq(GHz) | Return loss(dB) | Resonant freq (GHz) | Return loss(dB) | Resonant freq (GHz) | Return loss | Resonant freq (GHz) | Return loss(dB) |
| 4.49 | -24.45 | 4.54 | -12.41 | 5.25 | -14.08 | 5.55 | -19.53 |
| 5.14 | -19.36 | 5.00 | -22.02 | 6.13 | -14.22 | 6.14 | -22.56 |
| 5.53 | -14.34 | 5.35 | -17.01 | 6.50 | -19.71 | 6.54 | -28.99 |
| 6.52 | -30.6 | 5.64 | -21.13 | 7.43 | -26.68 | 7.44 | -18.79 |
| 6.88 | -11.51 | 5.98 | -13.2 | 8.16 | -17.37 | 8.17 | -15.50 |
| 7.33 | -27.10 | 6.34 | -14.75 | 8.43 | -20.07 | 8.47 | -14.13 |
| 8.2 | -19.64 | 6.76 | -24.46 | 9.37 | -21.64 | 9.35 | -11.84 |
| 8.53 | -8.80 | 7.60 | -20.96 | | | | |

VI. CONCLUSION

In order to create the fractal linear array for the second iteration of the Sierpinski carpet fractals, a linear array and a linear array of 8 elements were created. With 0.68 beam diameter and multi-band software, the linear array of 8 elements has a gain of 6.6 dB. The large linear fractal array beam is 0.67 to 0.4 with a 6.6dB to 7.7dB rise of the fractals. The degree of a side lobe is greater than the standard -13.5dB. The linear array's first side lobe level is -15dB. In the linear fractal series, the first lobe level is -14.6dB. There is no variation in the theoretical information of the experimental test performance.

A linear array is being designed and studied using fractal arrays based on Sierpinski geometry and the autonomic function of the geometry in multifaceted applications has been developed. In multiband efficiency, return loss, VSWR and gain are presented.

The 8 linear element array, fractal linear array, and E5071C vector network analysers have been

planned, simulated and evaluated. The second version of Sierpinski carpet fractals creates a new fractal series. The details seen in the figure can be seen. A linear array of 8 elements has an inclusion of 6.6 dB and a beam diameter of 0.68 and multiband features from 6.8 to 6.23. The linear beam diameter of the fractals is loosened from 0.68 to 0.54 with the gain increase from 6.6dB to 7.7dB. The linear array's first sidelobe is 0.15 dB, which is higher than the normal -13.5 dB sidelobe stage. The fractal linear array's first side lobe stage is -14.6dB.

There is a minor deviation from that of theoretical values in the findings of experimental analysis. This variations are due because of measurements in anechoic chamber speed made in open laboratory.

In the current work, an assortment of multiple fractal types of different dimensions may be modelled as well. This activity can be used to build antennas such as planar structures with controlled parameters

REFERENCES

1. Balanis C.A. *Antenna Theory: Concept Review 2*, Willy 1997.
2. B. B. Mandelbrot, *Nature's Fractal Geometry*. W H.Freeman, New York, 1983.
3. Y. Kim and D. Kim and D. The random array, L. Jaggard, *Proc. IEEE*, Vol.-IEEE, Vol. Nr. 5, pp. 647. 74, No. 9, pp.
4. D. H. Werner, et al., *Fractal antenna Array Theory and Architecture*, in *Electromagnetics Frontiers*,
5. D. H. Advertisements and R. Mittra, publishing company, NewYork, pp. 94-203. John Wiley & Sons, 2000.
6. D. Head and P. H. Werner, R. L. L. Werner, *Fractal Antenna Engineering: IEEE Antennas Propagation theory and construction of fractal antenna arrays*. Vol. 41, No. 5 of October, October 99, pp. 1009-1015.
7. "Fractal Components and Clusters" A ppled wireless and microwave, X. Yang, J. Chiochetti, D. Papadopolous, L.Suman
8. Douglas H.Werner and Suman Gangulli, *IEEE Antennas and Propagation Magazine "An Outline of Fractal Antenna Engineering Science."* Flight. NO, 45. I am dated February 2003
9. Tao Yun, Lie-Wei Li, Tapper Antenna Design's "A Noval collection," *Antennas and Wireless Literature. Flight. Seventh*, pages 362-365,2008.
10. Kim Y.-Kim Y. And Jaggard D.L., "Random Fractal Collection," *Proc. IEEE*, Vol.-IEEE, Vol. 74, row 1278-1280, 1986. 1986.
11. Kravchenko V.F., "Fragmentation Antenna Theory" and Strategies IVth Inter. Antenna Technology IV. Business, Vol. 1, pages 183- 189,2003. 1.
12. K.J.-K.J. Falconer, *Mathematical Foundering & Implementation "Fractal Geometry: Mathematical Foundations."*
13. C F Kai Fong Lee and Kwai Man Luk, Imperial College Press, 2011: *Microstrip Patch Antennas*.